An Automatic 3D Ultrasound and Photoacoustic Combined Imaging System for Human Inflammatory Arthritis

Xiaorui Peng, Aaron Dentinger, Shivangi Kewalramani, Zhanpeng Xu, Steven Gray, Soumya Ghose, Yew Teck Tan, Zhaoyuan Yang, Janggun Jo, David Chamberland, Guan Xu, Nada Abdulaziz, Girish Gandokota, David Mills, and Xueding Wang

***Abstract*—Aiming at a point-of-care device for rheumatology clinics, we developed an automatic 3D imaging system combining the emerging photoacoustic imaging with conventional Doppler ultrasound for detecting human inflammatory arthritis. This system is based on a commercial-grade GE HealthCare (GEHC, Chicago, IL) Vivid™ E95 ultrasound machine and a Universal Robot UR3 robotic arm. This system automatically locates the patient's finger joints from a photo taken by an overhead camera powered by an automatic hand joint identification method, followed by the robotic arm moving the imaging probe to the targeted joint to scan and obtain 3D photoacoustic and Doppler ultrasound images. The GEHC ultrasound machine was modified to enable high-speed, high-resolution photoacoustic imaging while maintaining the features available on the system. The commercial-grade image quality and the high sensitivity in detecting inflammation in peripheral joints via photoacoustic technology hold great potential to significantly benefit clinical care of inflammatory arthritis in a novel way.**

***Index Terms*— photoacoustic imaging, Doppler ultrasound imaging, inflammatory arthritis, automatic scan, three-dimensional imaging**

This research is supported by National Institute of Health under grant number R01AR060350.

Xiaorui Peng, Shivangi Kewalramani, Zhanpeng Xu, Janggun Jo, Guan Xu, and Xueding Wang are with the Department of Biomedical Engineering, University of Michigan, Ann Arbor, MI 48109, USA (e-mail: xiaoruip@umich.edu; shivi@umich.edu; zhanpeng@umich.edu; janggunj@umich.edu; guanx@med.umich.edu; xdwang@umich.edu).

Aaron Dentinger, Steven Gray, Soumya Ghose, Yew Teck Tan, Zhaoyuan Yang, and David Mills are with General Electric Research, Niskayuna, NY 12309, USA (e-mail: dentinge@ge.com; steven.gray@ge.com; soumya.ghose@ge.com; yewteck.tan@ge.com; zhaoyuan.yang@ge.com; millsda@ge.com).

David Chamberland and Nada Abdulaziz are with the Division of Rheumatology, Department of Internal Medicine, University of Michigan, Ann Arbor, MI 48109, USA (e-mail: davicham@umich.edu; nabdulaz@med.umich.edu).

Girish Gandikota is with the Department of Radiology, University of Michigan, Ann Arbor, MI 48109, USA (e-mail: ggirish@med.umich.edu).

I. Introduction

RHEUMATOID arthritis (RA), with a worldwide prevalence rate of 0.5%, is a chronic autoimmune disease that can be painful and lead to severe joint damage and consequent disability and inability to work [1, 2]. RA causes articular cartilage destruction due to inflammation of the tendon and connective tissues, and induces bone erosion in its later phase [3]. While RA is a severe, potentially crippling, and commonly disabling disease, effective and optimized therapy is hindered by the lack of cost-effective and robust joint imaging technology. Early initiation and timely adjustment of aggressive treatments that prevent disease progression, limit morbidity, and achieve faster remission requires diagnostic technologies sensitive to detecting pathological change and response to treatment. In clinical practice, rheumatologists rely on x-ray radiography, gadolinium-enhanced magnetic resonance imaging (MRI), and color Doppler ultrasound (US) as the leading imaging technologies for assessing RA. X-ray-based scoring methods [4, 5] are dependent on the identification of bone erosion and joint space narrowing, and are not sensitive to early functional changes noted in soft synovial tissues [6, 7]. MRI is excellent in imaging soft tissues. However, the high cost, long scanning time, need for intravenous contrast agents, lack of broad availability, and lack of portability all limit the use of MRI for treatment evaluation of RA [8]. Doppler US imaging can offer high-resolution images of joint structures and high sensitivity in detecting blood flow. Doppler US, however, is more sensitive to the fast blood flow in relatively large vessels. In contrast, slow blood flow in smaller capillaries, which are more clinically and pathologically relevant to early active synovitis, could be missed [9].

Recently, the emerging photoacoustic (PA) imaging technique, with intrinsically high sensitivity to light-absorbing molecules, especially hemoglobin in blood vessels, has been explored for its potential use in detecting and grading soft-tissue inflammation associated with arthritis. Real-time simultaneous PA and US imaging of human finger joints was achieved by integrating a laser system into a commercially available research US platform (Verasonics) equipped with a GPU card [10]. Later, this system was tested on a cohort of 26

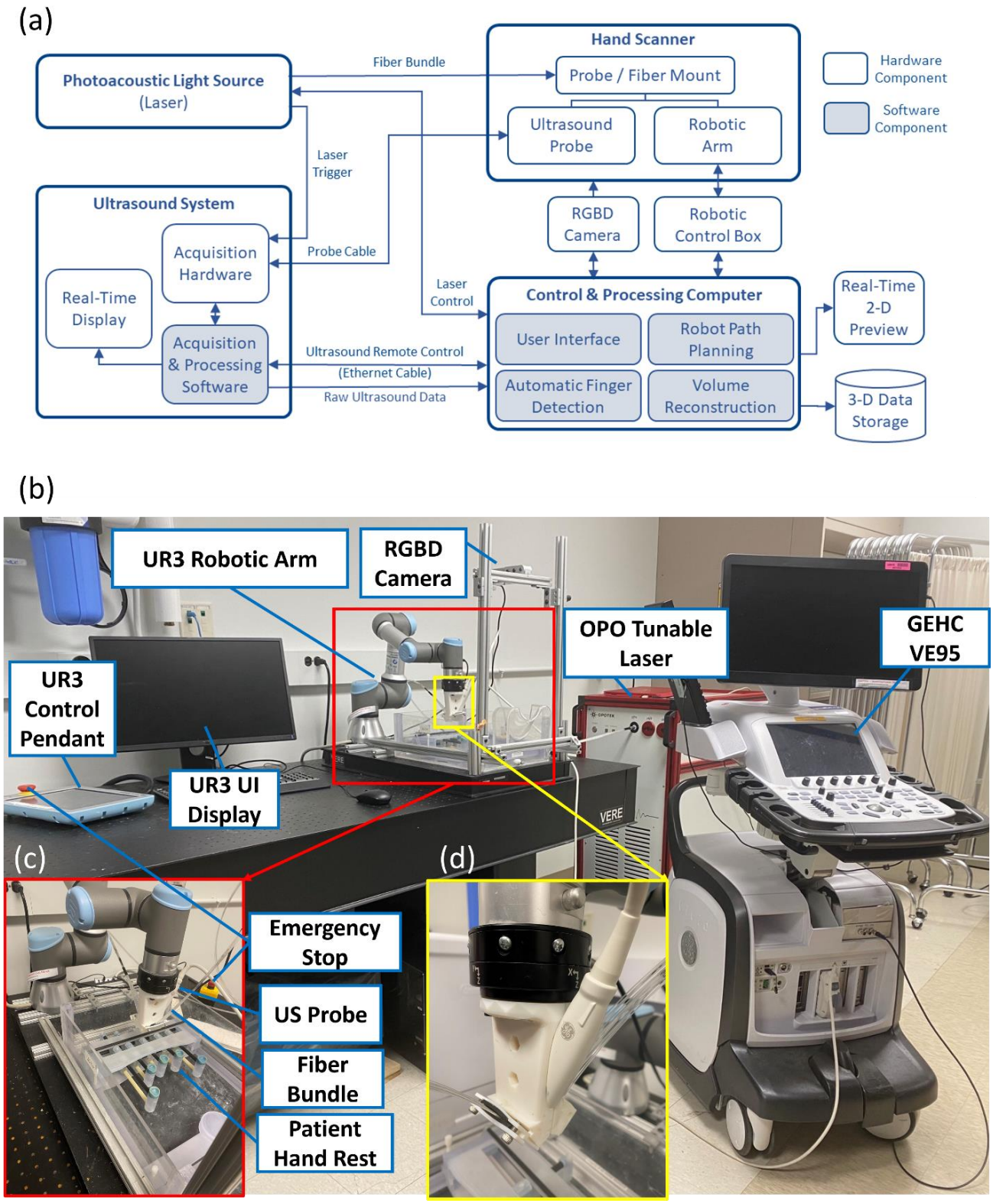

Fig. 1. (a) System block diagram. Photo of (b) the imaging system, (c) the imaging probe holder, robot arm, water tank and patient handrest, and (d) the probe holder with US probe in the middle and a fiber bundle on the side.

human subjects affected with RA, which validated that PA imaging was capable of detecting hyperemia (increased blood flow) and hypoxia (decreased blood oxygen saturation), two critical physiological biomarkers of synovitis reflecting the increased metabolic demand and the relatively inadequate oxygen delivery in affected synovium [11]. Later, an LED-based PA imaging system was employed to identify inflammatory arthritis in human hand joints, and demonstrated that PA imaging, with a higher sensitivity to angiogenic microvascularity, is more sensitive in detecting subclinically

active arthritis compared to Doppler US imaging [12]. Also, using the same LED-based PA imaging system, a study on ten patients with seronegative spondyloarthropathy (SpA) validated that PA imaging is sensitive in detecting enthesitis in Achilles tendons [13]. In a recent study on a cohort of 31 RA patients, PA imaging was facilitated by a commercially available clinical US device (Resona 7, Mindray Bio-Medical Electronics Co., Ltd.), which demonstrated that PA scores have significant correlations with standard clinical scores for RA, and that PA imaging measured oxygen saturation (SO2) patterns are also associated with clinical scores that reflect pain severity [14]. In another recent study on a large cohort of 118 patients with RA and 15 healthy control subjects, it was validated that the hypoxia detected by PA imaging in thickened synovium correlates with less vascularization and higher disease activity in RA patients [15]. The findings from these pioneering clinical studies are encouraging, suggesting that PA imaging holds great potential to be developed into a new diagnostic tool for rheumatology clinics, especially when combined with established Doppler US imaging methods.

To facilitate quick translation to the rheumatology clinic, PA imaging of human joints and tendons should show clinical-grade image quality. More importantly, the functional measurements from PA imaging reflecting the severity of RA, including hyperemia and hypoxia, should be quantitative and highly reproducible. In previous developments of PA imaging targeting RA, PA images were acquired from 2D imaging planes of the joints affected by arthritis. Similar to the situation in 2D Doppler US imaging, measurements from 2D PA imaging are highly dependent on the position and orientation of the imaging probe and the pressure that the probe puts on the target joint. Consequently, 2D PA imaging outcomes have large inter-operative and intra-operative errors and are also difficult for other research groups or clinics to repeat, which hinders the clinical translation of this promising technology.

In this study, we work towards a point-of-care 3D automatic PA and US dual-modality imaging device for RA. This system uses commercial-grade signal acquisition and image processing of a GE HealthCare (GEHC) VividTM E95 (VE95) US machine and achieves high-quality real-time PA imaging and Doppler US imaging with 3D volumetric reconstruction in post-processing. The automatic acquisition of PA and Doppler US images is enabled by an overhead camera and the use of algorithms to automatically identify the finger joints of a free-positioned hand on an adjustable stage and a robotic arm that can automatically scan the US probe across the target joint to enable 3D imaging. The goal of this highly automatic feature is to reduce inter-operative and intra-operative errors and enable quantitative and reproducible imaging results. Moreover, unlike 2D PA and US images that are susceptible to scanning parameters and operator skills, 3D images allow volumetric measurements in the joint with the goal of superior accuracy and reproducibility. Such a device, once validated, could be conveniently used in rheumatology clinics or other resource-limited environments, and can be operated by anyone after minimal training, without the need to involve a radiologist or sonographer.

II. Methods

A. System Overview

A block diagram of the 3D automatic imaging system for inflammatory arthritis is shown in Fig. 1a. The main hardware components consist of a light source, an ultrasound imaging system capable of PA imaging, a robotic arm with control hardware, a video camera and computer for controlling the components and processing the data. Fig. 1b shows a picture of the prototype imaging system developed for 3D automatic imaging of inflammatory arthritis. A Nd:YAG laser pumped OPO (Phocus MOBILE, OPOTEK Inc.), coupled to a custom-made fiber bundle (CeramOptec) with 36 800-µm fibers as input and bifurcates into 2 outputs with an equal number of 18 fibers each, was used as the PA light source. This tunable laser system used as the illumination source for PA imaging has a repetition rate of 10 Hz and a pulse width of 5 ns. The ultrasound system consisted of a GEHC VE95 cardiovascular system with a L8-18i-D high-frequency linear probe. The commercially-available ultrasound hardware was unchanged, while modifications were made to the acquisition and processing software to enable real-time simultaneous B-mode and PA imaging.

The optical design utilizes a custom 3D-printed fixture to mount the ultrasound probe and the fiber bundles on the Universal Robots (UR) Robotic Arm (UR3), as shown in Fig. 1d. The fiber bundles are offset from the probe as shown in Fig.1c. The probe surface is positioned 1-2 cm away from the hand joint, and the water between the probe surface and hand joint surface works as the acoustic coupling materials. The use of a water bath for acoustic coupling provides an unobstructed path for the light to evenly illuminate the entire finger. As another advantage, based on their different arriving time, the useful PA signal from the joint anatomy can be easily separated from the PA signal induced by the light absorption at the probe surface which can cause artifacts in PA images.

The UR3 robotic arm and the RGBD camera (Intel RealSense Depth Camera D435) are secured to a water tank equipped with a handrest to reduce motion and improve subject comfort during the 3D scan. A Linux computer coordinates the control of all the hardware components for the automated acquisition including providing user interface for the acquisition, automatically locating the finger joints for the operator, planning, and controlling the robotic scan, receiving ultrasound image data from the ultrasound system, and reconstructing spatially registered volumes from B-mode and PA images as well as B-mode and color Doppler images.

B. Real-Time Photoacoustic Imaging

We have configured a new PA imaging mode on the VE95 US unit to receive a trigger from the tunable laser, so the receive signal processing chain starts without a transmit event from the US unit. We have modified the VE95's parallel delay-and-sum beamforming code for one-way ultrasound

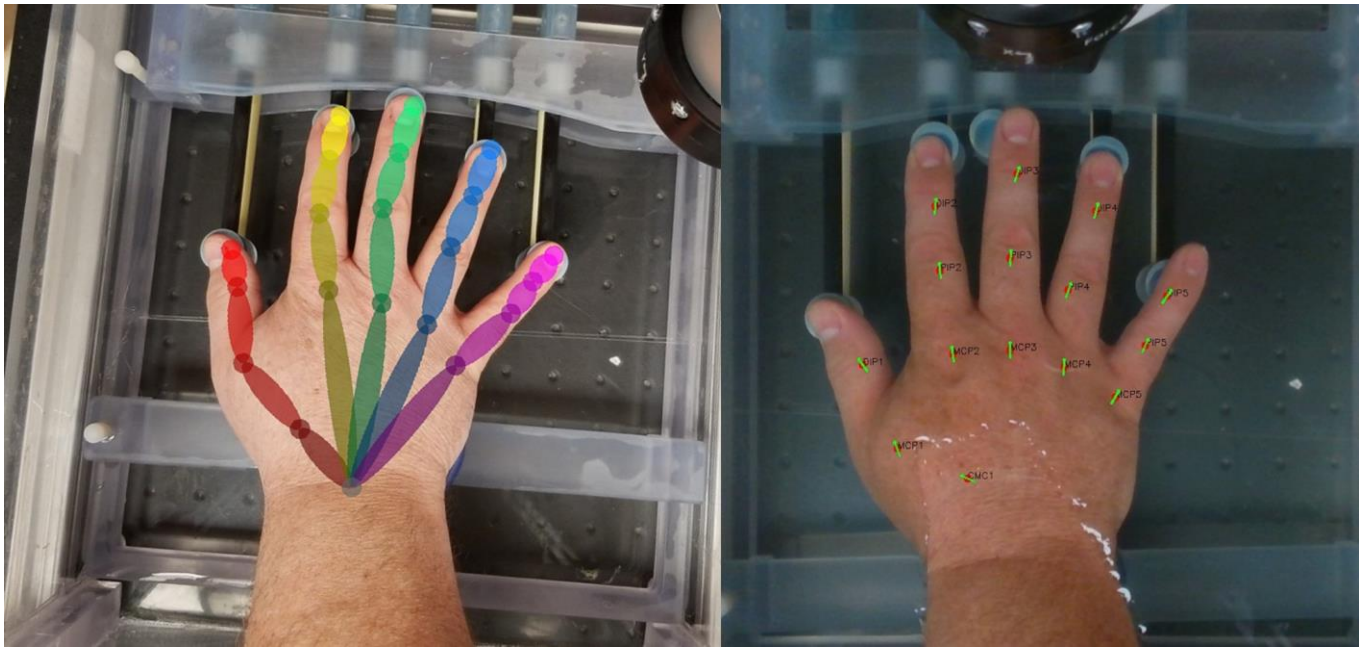

Fig. 2. (left) twenty-one hand keypoints estimated by OpenPose library. (right) Fifteen estimated joint locations are used for imaging of inflammatory arthritis.

propagation of the PA signal, instead of the typical two-way processing for B-mode and color Doppler imaging. A bandpass filter is then applied to the beamformed signal with the center frequency and bandwidth selected from the VE95's control panel. We then create an image using the power of the beamformed PA signals following a single laser pulse illumination. We implement the new PA imaging as a duplex mode by interleaving US B-mode imaging pulses acquired with the same transducer array between each PA laser firing to provide a structural image that is spatially registered with the PA image. A combined image is constructed with the PA image overlaid on the B-mode image, similar to power Doppler imaging, and is displayed on the VE95 during live scanning.

For superficial imaging of small vessels in the finger joints, the image acquisition was optimized to provide the finest resolution by preserving highest frequencies of the broadband PA signals. Since there is no ultrasound transmit beam in PA mode, the lateral and axial resolutions of the system depend only on the receive beamforming parameters. The active receive aperture in the receive beamforming was adapted with depth for constant f-number imaging with 128 receive beams formed in parallel across the physical aperture. The center frequency and bandwidth of the temporal receive filter applied to the one-way beamformed PA signal were selectable on the system with the center frequency ranging from 5.0 MHz to 12.5 MHz and the bandwidth ranging from 1.0 MHz to 4.0 MHz. For the PA images shown, the receive center frequency was 12.5 MHz, the receive bandwidth was 3.8 MHz, and the receive f-number was 1.4 resulting in a receive beamwidth of approximately 200 µm and an axial resolution of approximately 400 µm. Additional details regarding the spatial resolution of this imaging system as well as other system parameters can be found in Supplementary Materials.

The PA image output by the system is formed from the envelop of the received signal that is log compressed and displayed on a 40 dB of dynamic range. The gain knob on the system control panel in the PA mode operates similar to the gain know in traditional power Doppler and provides the ability to adjust amplification of the received signal. For the *in vivo* data collection, the gain was adjusted by the operator based on the PA signal strength to avoid saturation of the peak signal and excessive amplification of electronic noise. The implementation allows for additional post-processing of the PA images, including spatial and temporally averaging, with the parameters accessible to the operator through the user interface. For all 3D imaging modes, the temporal frame averaging was turned off to eliminate blurring of the data in the direction of the robot motion. For the *in vivo* images with sufficient PA signal strength, as shown in Figure 5, the lateral and axial smoothing setting was also turned off to maintain the highest spatial resolution.

The sensitivity of the PA acquisition system was characterized experimentally using a single element piston transducer submerged in a water bath to simulate a PA source. The piston transducer was placed at a depth of 2 cm and aligned to point directly at the GEHC L8-18i-D probe just below the water's surface. A function generator was used to produce a short ultrasonic burst at 12 MHz from a piston transducer. The gain on the ultrasound system was adjusted so the signal from the piston transducer was just below the saturation level on the PA display. Then, the voltage of the input waveform reduced until the noise level in the reconstructed PA image was approximately equal in magnitude to the signal from the piston transducer (SNR $\approx$ 0 dB). Next the GEHC L8-18i-D was replaced by a calibrated hydrophone to measure the pressure incident on the probe. A minimum detectable incident pressure of 370 Pa was measured for the lowest voltage setting.

C. 3D Robotic Scanning and Volume Reconstruction

To realize 3D imaging of a target finger joint, the imaging system uses a UR3 robotic arm for scanning the probe over the

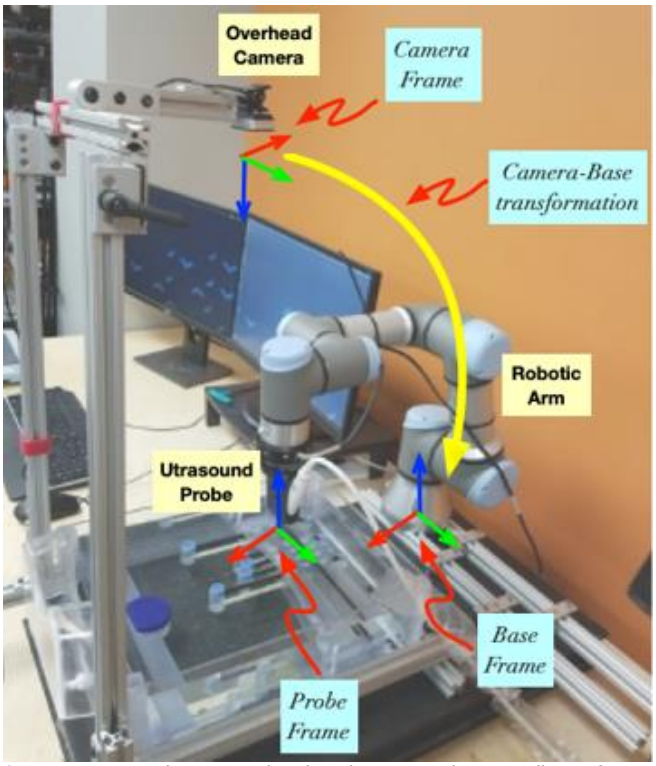

Fig. 3. Integrated system showing the respective coordinate frames and the camera-base transformation.

joint. For added safety, a force-torque sensor (Robotiq FT300) is mounted to the end of the UR3 arm. We have designed a 3D-printed mount which attaches to the force-torque sensor and holds both the US probe and the fiber bundle. The UR3 is mounted onto a base that also holds the mount for the RGBD camera and the water tank containing a patient handrest. This handrest allows individual adjustment of each finger placement to facilitate comfort and the required positioning and stillness for scanning. The water bath serves as the acoustic coupling between the probe and the tissue with the fingers resting approximately 2 cm below the water's surface, while the ultrasound probe is only submerged to about 0.5 cm for the 3-D scan. In this setup, the probe does not contact the tissue and, therefore, does not cause any tissue deformation during the 3-D scan.

On the software side, we use the open-source Robotics Operating System (ROS) and ROS tools [16] on the control computer to handle inter-process communication, visualization, user interface, arm kinematics, and collision checking. For the UR3, we use the manufacturer-provided robotic arm programming script, URScript [17], and custom US control and streaming code.

For patient safety, an emergency stop (e-stop) button is accessible to the patient. Pressing this will pause the scan, which can be resumed once the operator clears the e-stop. The operator also has access to their own e-stop, which is part of the UR3 control pendant. For additional safety, the force on the probe is monitored by the force-torque sensor and relayed to the control computer. The control computer uses a 3 N threshold to detect contact and abort the scan. The face of the probe has an area of 13 mm×36.9 mm=479.7 mm^2 or 4.797 cm^2. In case of an impact at 3 N, the pressure spread over this surface and applied by the probe is 3 N / 4.797 cm^2=0.625 N/cm^2. For comparison, according to the workplace safety guidance (RIA TF R15.606-2016, Table A.2 on Biomechanical limits), the maximum allowable force for a forefinger is 140 N. The maximum allowed pressures for forefinger pads and joints range from 220 to 300 N/cm^2.

Different scan trajectories are required to gather clinically relevant data. These are composed of different primitives, such as linear and arc segments, and different velocity profiles. In this work, we have focused on linear scans for the 3D PA imaging. This scan type takes in a target center location and relative probe pose, as well as scan length, direction, speed, and acceleration. It assumes a trapezoidal velocity profile, starting at zero, ramping up at a constant acceleration to a maximum velocity, maintaining that velocity, then ramping down again at a constant deceleration. The trajectory length is extended at the beginning and end, so the entire clinician-specified joint segment is in the constant velocity section.

The Linux computer controls the robotic scanning and synchronizes the ultrasound data acquisition on the VE95 through a remote connection over an ethernet cable. The image sequences acquired with the VE95 are streamed to the robot control computer over the ethernet cable for storage with the robot and ultrasound acquisition parameters. These image sequences are then processed to extract the 2D frames corresponding to the robot scanning period. The parameters from the robot trajectory are used to create spatially registered 3D data files with the correct Cartesian geometry for each imaging modality.

D. Automatic Finger Joint Detection

University [18, 19]. This is a GPU-accelerated deep-learning algorithm that operates on 2D imagery to provide joint locations within that 2D image. Given an overhead capture of a 2D hand image, the OpenPose library performs twenty-one hand keypoint estimations using a pre-trained deep-learning model, as shown in Fig. 2 (left). For detecting inflammatory arthritis, only 15 joint locations are extracted from the resultant hand key points and labeled accordingly with their respective joint names, as shown in Fig. 2 (right). We use the aligned 2D and depth imagery from the RealSense RGBD camera to project a ray from the camera through the image plane and find the intersection with the depth image. This results in the 3D location of the joints with respect to the camera frame.

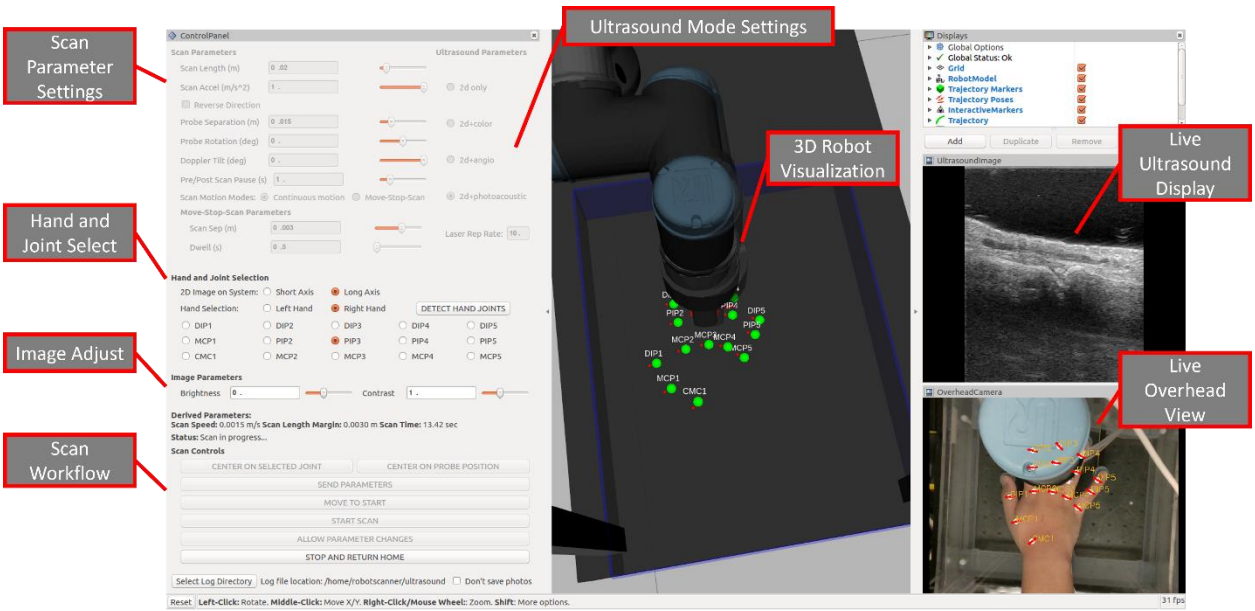

Fig. 4. The user interface for the automatic 3D PA and US scanning system. The live ultrasound display and live overhead view are updated in real time. The 3D robot visualization moves with the scan. The detected hand joint locations are visible.

To position the US probe for scanning a target joint in the workspace, the relative poses of the camera and the robotic arm's base must be known. This is achieved by calibrating the camera frame against the robotic arm's base frame, as shown in Fig. 3. The calibration is accomplished by gathering images of the robot arm attached to a checkerboard fixture as it visits multiple known configurations across the workspace. Nonlinear least-squares optimization is then used to solve for the transformation between the camera frame and the robotic arm's base frame [20]. The US probe frame (location of the US probe in the workspace), with respect to the robotic arm's base frame, can be calculated using the robotic arm's joint lengths and angles. The resultant information allows the estimated 3D hand-joint locations to be transformed with respect to the base frame, thus, allowing the US probe to be positioned at the desired location within the workspace for scanning.

E. System Operation

User Interface – As shown in Fig. 4, the user interface has been designed to guide the operator in performing a linear scan. Scan parameter settings and imaging mode selection are presented on the top left of the screen. Hand and joint selection for use with automatic hand joint detection occupy the middle left, with image adjustments that may affect the detection just below. The bottom left of the interface has program flow buttons to trigger the next step in the underlying state machine governing the system's operation. Similar to parameter settings, only the buttons for valid transitions to another state are enabled, and the rest are grayed out. As with the buttons, scan parameters are grayed out when unavailable.

The middle of the interface is a 3D visualization of the robot and enclosure. While this display does not update with a live view of the patient's hand (the live view is a 2D video on the bottom right of the user interface), it shows the 3D position of the detected joints. It is used to preview the scanning motion for the clinician to accept, modify, or decline prior to scan execution. The top right of the user interface shows a list of devices and connection status, with ultrasound and camera images under that list. While the scan is in progress, the live ultrasound display on the middle right updates in real time.

Positioning – Operation begins with the patient submerging their hand in the water and placing it atop the handrest. The operator then sets the center position of the scan, which can be done through an automatic hand joint detection process or manually repositioning the robot arm.

For automatic positioning, after the patient places their hand on the handrest, the RGBD image from the overhead camera is used for automatic hand joint detection. By selecting the 'Hand and Joint Selection' panel and clicking the 'Detect Hand Joints' button on the left of the user interface, as shown in Fig. 4, the hand joints labels appear in the overhead image on the bottom right and in the central 3D view showing the robot as well. The 3D view is useful for the operator to detect if a joint has been placed spuriously. If so, the process may be repeated to correct the spurious positioning, or the operator may opt to fall back to the manual approach.

For manual positioning, the operator holds the button on the UR3 control pendant to place the robotic arm in gravity-compensated mode, allowing the arm to be positioned freely. While holding the button and pendant with one hand, the operator uses the other hand to place the robot such that the US probe is centered above the scan region of interest.

Regardless of the positioning method, the operator uses the user interface on the control computer to set parameters relevant to the scan, including scan speed, acceleration ramping, and length. These parameters are sent to the planning module, and the resulting plan is displayed in the user interface for the operator to either confirm or modify. The operator hits the start button on the user interface, and the robot moves horizontally to the start location; it then performs the scan using the parameterized motion profile. At the end of the scan, the robot moves horizontally away from the patient to its home position. Each scan generates a timestamped log file with scan parameters and probe positions with respect to the robot base coordinate frame for use in correlating robot positions with gathered imaging data.

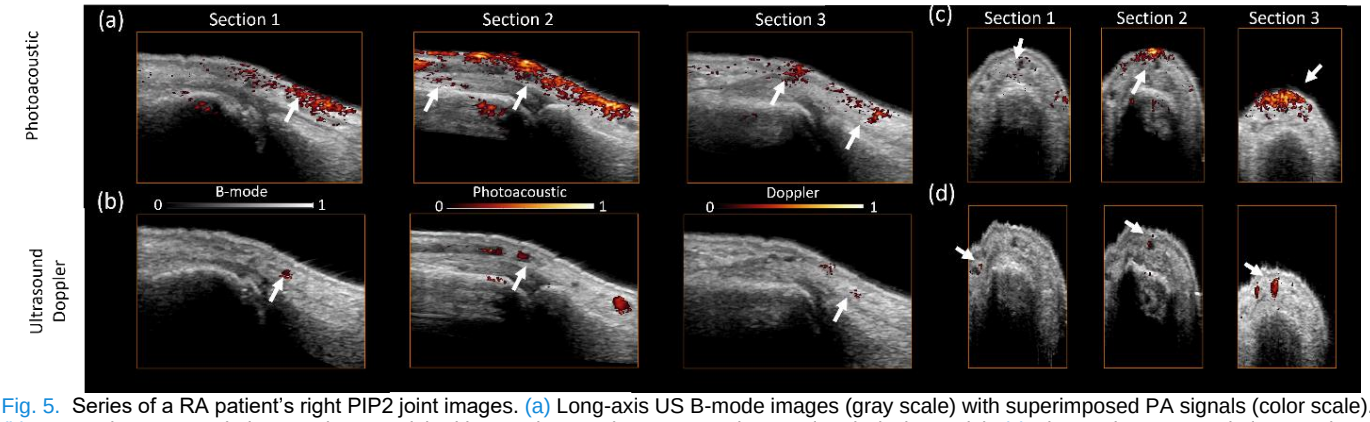

Fig. 5. Series of a RA patient's right PIP2 joint images. (a) Long-axis US B-mode images (gray scale) with superimposed PA signals (color scale). (b) Long-axis US B-mode images (gray scale) with superimposed power Doppler US signals (color scale). (c) Short-axis US B-mode images (gray scale) with superimposed PA signals (color scale). (d) Short-axis US B-mode images (gray scale) with superimposed power Doppler US signals (color scale). White arrows mark the hyperemia area in PA and the large vessels in Doppler.

Adjustable Parameters – The operator can specify the imaging mode for data collection, choosing from B-mode US only or B-mode US plus one of the following: color flow imaging (color or power Doppler US imaging mode) or PA imaging. When performing B-mode US with and without PA imaging, the robot moves continuously along the scan trajectory as images are acquired. When performing B-mode US with one of the Doppler US modes, the robot will move to the next location in the trajectory, stop, acquire images, and repeat. The robot needs to follow the move-stop-scan fashion for Doppler US imaging modes to avoid imaging artifacts from the probe motion.

Different parameters determine the movement of the robot and the scan direction. The overall scan length is determined by the scan length parameters. The scan acceleration parameter sets the acceleration from rest to the constant scan velocity and the later deceleration back to zero velocity after the scan is complete. In the linear scan mode, a constant scan velocity is maintained over the desired scan length, with the scan velocity determined to provide adequate spatial sampling of the anatomy in the direction of the motion. This is accomplished by setting a fixed separation (relative to the US beam width in the robot scan direction) between the slices in the 3D data and then calculating the required scan velocity based on the US frame rate. Reverse direction helps to change the direction of the scan, and probe separation sets the distance between the probe and the joint. Scans can also be carried out in a perpendicular direction, and probe rotation helps to achieve this. The pre/post scan pause gives the US unit some time to start streaming. Scan motion mode determines whether the probe should move continuously while scanning or should move-stop-scan. Move-stop-scan also has sub-parameters which are the scan length (distance between the scans) and dwell time (how long to stop for each scan).

III. Results

The performance of this automatic 3D PA and US dual-modality imaging system for arthritis was initially evaluated on RA patients. All procedures in this study were approved by the Institutional Review Board of the University of Michigan Medical School (HUM00003693). Informed consent was obtained from all subjects. The RA patients involved in this study were men and women over 18 years old, with apparent swelling and pain in at least one of their finger joints. The patients were recruited, and their pathologic conditions were confirmed by certified rheumatologists at the University of Michigan Rheumatology Clinic following the American College of Rheumatology (ACR) criteria.

For PA imaging, we used a laser wavelength of 750 nm with an applied energy density of 20 mJ/cm^2 on the skin, which was lower than the ANSI safety limit of 25.2 mJ/cm^2 for skin exposure. 750-nm wavelength was chosen for PA imaging because our Nd:YAG laser pumped OPO has the maximal and stable energy output at this wavelength. Considering the tradeoff between the penetration depth and the optical absorption for hemoglobin, this wavelength is appropriate for PA imaging of human fingers with a targeted imaging depth of <2 cm. For US B-mode and Doppler mode, the imaging parameters are based on the Small Parts application on the Vivid E95 commercial software suitable for musculoskeletal, vascular, and superficial anatomy. The imaging parameters, for both US B-mode with PA imaging and US B-mode with Doppler US imaging, were modified from the default values by the operator to optimize the image quality for a given patient. The targeted anatomy was located 1-2 cm from the probe, where the best resolution could be achieved. For the imaging results shown, the US B-mode was operated in harmonic mode with a transmit frequency of 7.0 MHz and receive frequency of 14.0 MHz. The receive center frequency and bandwidth for PA imaging was 12.5 MHz and 3.8 MHz, respectively. The transmit frequency for Doppler imaging was 7.2 MHz and the Doppler packet included 14 firings acquired at a pulse repetition frequency (PRF) of 1.0 kHz.

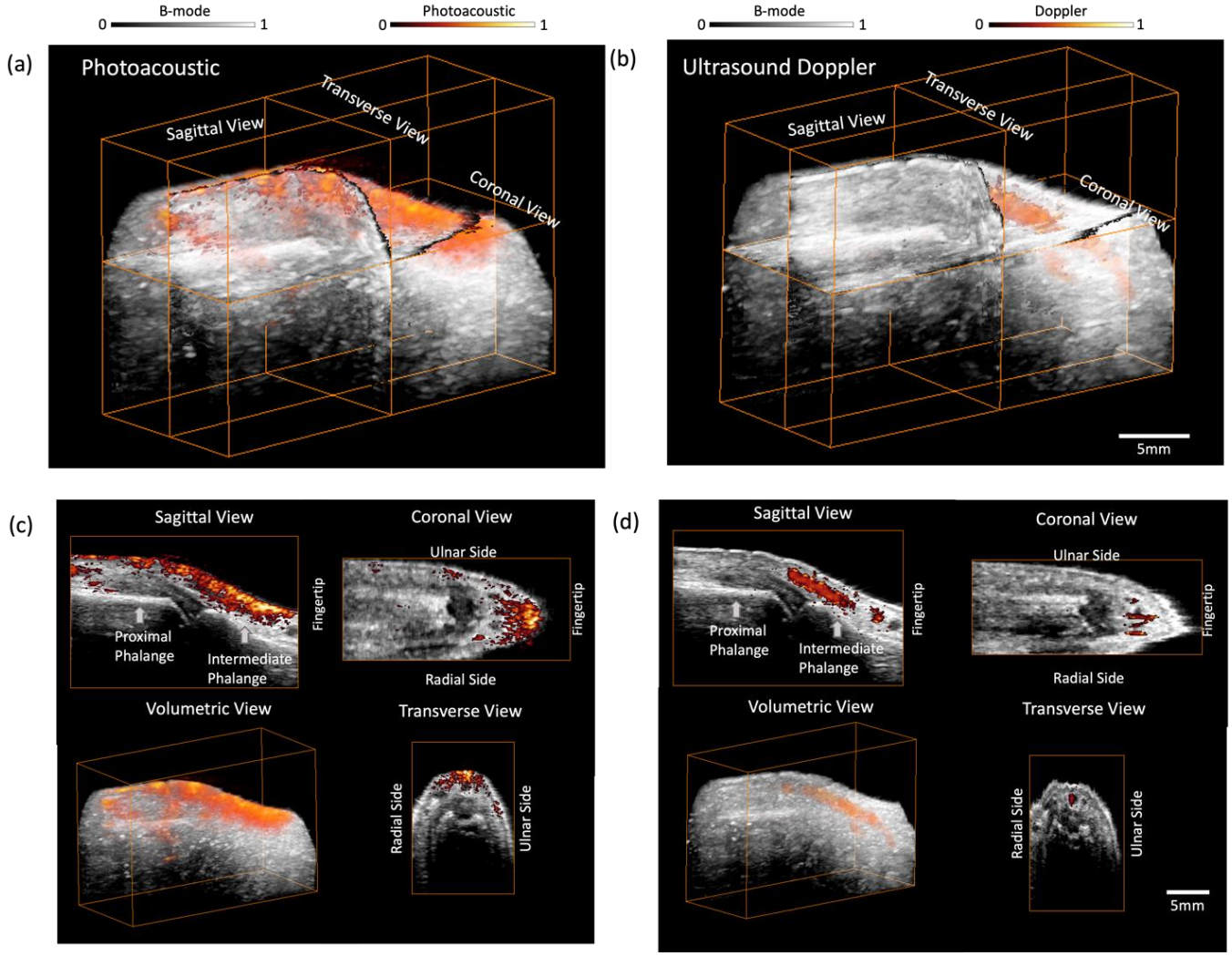

Fig. 6. 3D volumetric rendering of (a) the B-mode and PA image and (b) the B-mode and Doppler US image of a RA patient's right PIP2 joint. The 2D images along different views are shown in (c) and (d), where the plane for each view is marked in (a) and (b),.

Representative imaging results from a RA patient's right hand second proximal interphalangeal (PIP2) joint are shown in Fig. 5. The detailed demographic and clinical information of this patient can be found in the Supplementary Materials. Series of 2D images along the long-axis and short-axis of the joint are presented. In the PA image, besides strong signals from the skin, some strong signals can be noticed in areas close to the phalanges. These signals reflect the hyperemia associated with microvessels as a biomarker of RA-induced soft-tissue inflammation [11]. In the Doppler US images, we can see enhanced flow in several large superficial vessels close to the skin, which confirms the active synovitis in this joint. However, unlike the PA imaging, the Doppler US images are not sensitive to microvascular flow and did not show any activities in the areas close to the phalanges. Figs. 6(a) and (b) present the 3D volumetric rendering of the PA and Doppler US imaging results from the same joint; while Figs. 6(c) and (d) show the images along coronal, transverse, and sagittal views, as well as volumetric view. The Amira-Avizo software (Thermo Fisher Scientific) was used to visualize the volumetric data. The PA image in 3D volumetric rendering better shows the distribution of the hyperemia in the joint and their relative locations to the phalanges, large vessels, and skin. The 3D PA and Doppler US imaging results from another patient with RA can be found in the Supplementary Materials. In Fig. 7, some representative imaging results of a healthy control's PIP3 are provided. Both the PA signals and Doppler ultrasound signals in the joint of the healthy control are comparatively lower than those from the RA patients.

IV. Conclusion and Discussion

Encouraged by the promising results from several pioneering studies on RA patients, we are further advancing the translation of the emerging PA imaging technology to the clinical management of inflammatory arthritis. In this work, our goal is to develop a point-of-care joint imaging prototype that can enable early detection and early treatment modification, changing the current procedures in rheumatology clinics. An automatic 3D PA and US dual-modality system for imaging the peripheral hand joints of RA patients has been developed by modifying a GEHC VE95 US machine and integrating it with a tunable laser and a robotic arm. Through the designed user interface with an automatic hand joints identification method, multiple targeted joints in a

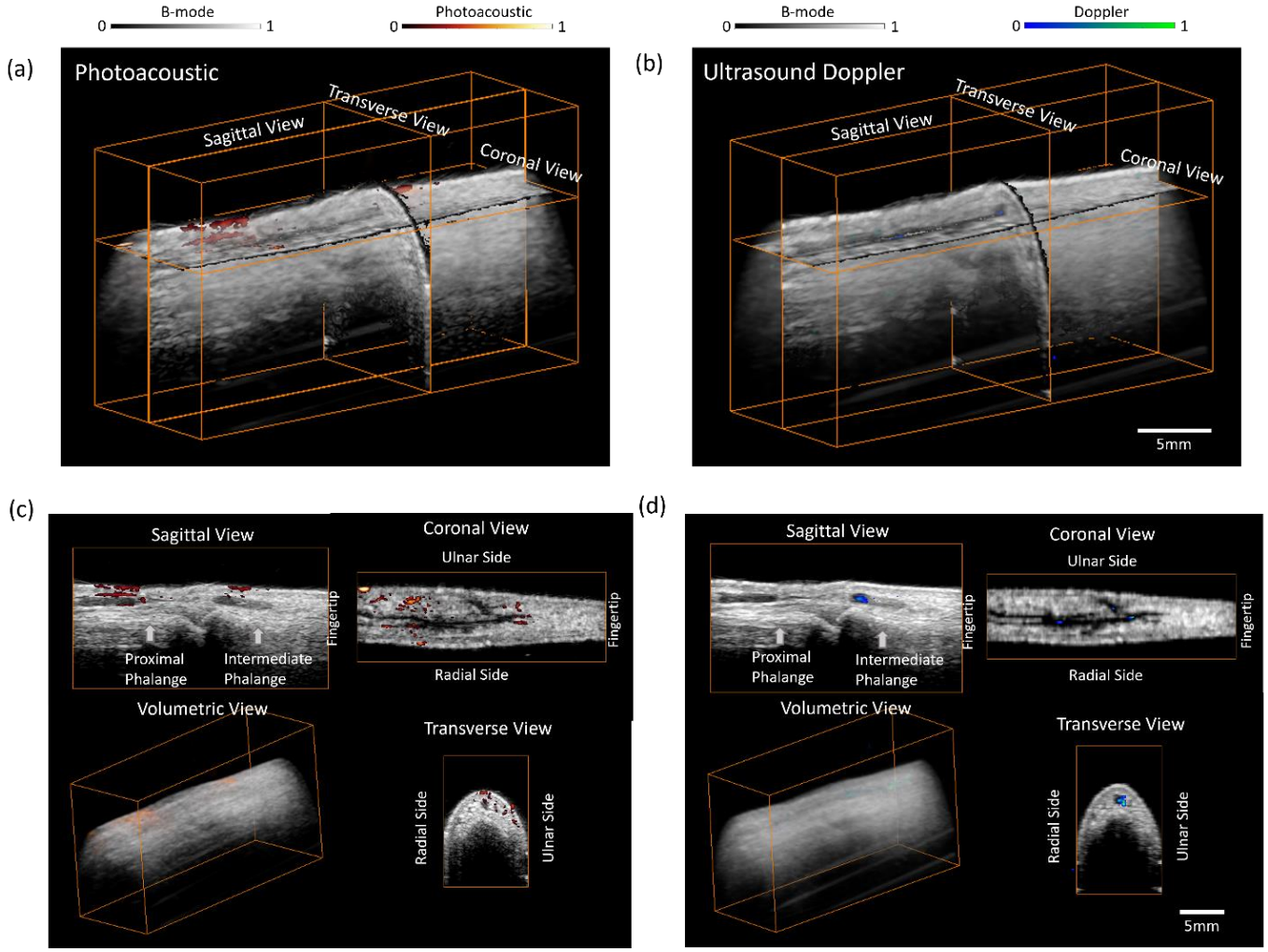

Fig. 7. 3D volumetric rendering of (a) the B-mode and PA image and (b) the B-mode and Doppler US image of a healthy control's right PIP3 joint. The 2D images along different views are shown in (c) and (d), where the plane for each view is marked in (a) and (b),.

free-positioned hand putting on an adjustable stage in the water can be identified automatically. Then an automatic scan of the targeted joints via the probe driven by the robotic arm can be realized to achieve 3D B-mode US imaging together with either the PA function or Doppler US function. Such a point-of-care device can be handled by any operator (with minimal training) without complete medical knowledge, which should lead to better acceptance in rheumatology clinics or other resource-limited environments. The 3D volumetric information provided by this automatic imaging system also helps make the functional measurements quantitative and reproducible, which may facilitate the comparisons between the outcomes from different studies and even from other sites in future clinical trials.

The performance of this system was examined via an initial study on RA patients with clinically confirmed inflammation in their finger joints. It was validated that the PA imaging function of this system could detect and display the hyperemia deep in the joints with good sensitivity and high image quality. The 3D Doppler US imaging function enabled by this system could also detect the enhanced flow due to the active inflammation in the joints. However, all the Doppler signals were from the large vessels, which were superficial in the digits, but none were from the hyperemia associated with microvessels deep in the joints. This matches with the findings from our previous studies suggesting that PA imaging, compared to conventional Doppler US imaging, could be more sensitive in detecting mild inflammation in the joints and tendons of arthritis patients [11-13].

The clinical value of this system and PA imaging technology, in general, will be further assessed in our future studies. One of our ongoing studies is to perform a quantitative comparison between PA imaging and Doppler US imaging via a longitudinal study in RA patients under pharmaceutical treatments. With both the PA imaging function and Doppler US imaging function facilitated by the same commercial grade GEHC VE95 US machine, this dual-modality system can enable a fair and objective comparison between the two modalities in terms of the pros and cons of each in detecting and grading soft-tissue inflammation.

As one of the limitations of this study, the current speed of this automatic 3D PA and US imaging system is not high. The 3D PA imaging function relies on continuous scanning to acquire volumetric results, which usually takes about 7.4 seconds to scan one joint. However, to avoid imaging artifacts from the probe motion, the 3D Doppler US imaging function employs the move-stop-scan fashion to acquire volumetric results. Thus, it takes up to 180 seconds to scan one joint

(depending on the setting parameters). We are working to address this limitation, although the current imaging speed is also acceptable for our ongoing study on patients.

Same as the procedure in clinical ultrasound assessment of peripheral joint inflammation of arthritis patient, our imaging system acquires images from a few targeted joints only, instead of from all the joints in the hand. In our imaging procedure, the user selects the target joints for imaging on the user interface, and then the robotic arm moves the probe to the target joints selected by the user. Then the user evaluates the probe positioning and proceeds with 3D image acquisition. Due to the anatomical complications in the peripheral joints of human hands, quality control is important for US imaging to detect morphological and functional changes indicating inflammation. Currently, we do not have an automated method to evaluate image quality during the scan of US and PA images. When it is determined that image quality may have been negatively impacted by an imaging artifact or poor anatomical access, a repeat scan can be performed. In the future, to enhance the automatic fashion of this imaging system, automatic scanning guided by an automatic method to evaluate image quality can be developed.

ACKNOWLEDGMENT

This research is supported by National Institute of Health under grant number R01AR060350.

REFERENCES

[1] D. Aletaha and J. S. Smolen, "Diagnosis and Management of Rheumatoid Arthritis: A Review," (in English), JAMA : the journal of the American Medical Association, vol. 320, no. 13, doi: 10.1001/jama.2018.13103.

[2] K. Almutairi, J. Nossent, D. Preen, H. Keen, and C. Inderjeeth, "The global prevalence of rheumatoid arthritis: a meta-analysis based on a systematic review," (in English), Rheumatology international, vol. 41, no. 5, doi: 10.1007/s00296-020-04731-0.

[3] "Paul-Ehrlich-Institute Researchers Highlight Recent Research in Disease Progression (Update on the Pathomechanism, Diagnosis, and Treatment Options for Rheumatoid Arthritis)," (in English).

[4] A. W. Visser et al., "Radiographic scoring methods in hand osteoarthritis--a systematic literature search and descriptive review," (in Eng), Osteoarthritis Cartilage, Research Support, Non-U.S. Gov't Review vol. 22, no. 10, pp. 1710-23, Oct 2014, doi: 10.1016/j.joca.2014.05.026.

[5] S. Boini and F. Guillemin, "Radiographic scoring methods as outcome measures in rheumatoid arthritis: properties and advantages," (in Eng), Ann Rheum Dis, Research Support, Non-U.S. Gov't Review vol. 60, no. 9, pp. 817-27, Sep 2001. [Online]. Available: http://www.ncbi.nlm.nih.gov/pubmed/11502606.

[6] M. N. Zeman and P. J. Scott, "Current imaging strategies in rheumatoid arthritis," (in Eng), Am J Nucl Med Mol Imaging, vol. 2, no. 2, pp. 174-220, 2012. [Online]. Available: http://www.ncbi.nlm.nih.gov/pubmed/23133812.

[7] E. L. Rowbotham and A. J. Grainger, "Rheumatoid arthritis: ultrasound versus MRI," (in Eng), AJR Am J Roentgenol, Review vol. 197, no. 3, pp. 541-6, Sep 2011, doi: 10.2214/AJR.11.679810.2214/AJR.11.6630.

[8] D. Chamberland, Y. Jiang, and X. Wang, "Optical imaging: new tools for arthritis," (in Eng), Integr Biol (Camb), Research Support, N.I.H., Extramural Review vol. 2, no. 10, pp. 496-509, Oct 2010, doi: 10.1039/b926506f.

[9] I. Goldie, "The synovial microvascular derangement in rheumatoid arthritis and osteoarthritis," Acta orthopaedica Scandinavica, vol. 40, no. 6, pp. 751-64, 1969. [Online]. Available: http://www.ncbi.nlm.nih.gov/pubmed/5376789.

[10] J. Yuan et al., "Real-time photoacoustic and ultrasound dual-modality imaging system facilitated with graphics processing unit and code parallel optimization," Journal of Biomedical Optics, vol. 18, no. 8, pp. 86001-86001, 2013.

[11] J. Jo et al., "A Functional Study of Human Inflammatory Arthritis Using Photoacoustic Imaging," Sci Rep, vol. 7, no. 1, p. 15026, Nov 3 2017, doi: 10.1038/s41598-017-15147-5.

[12] J. Jo et al., "Detecting joint inflammation by an LED-based photoacoustic imaging system: a feasibility study," J Biomed Opt, vol. 23, no. 11, pp. 1-4, Nov 2018, doi: 10.1117/1.JBO.23.11.110501.

[13] J. Jo, G. Xu, E. Schiopu, D. Chamberland, G. Gandikota, and X. Wang, "Imaging of enthesitis by an LED-based photoacoustic system," J Biomed Opt, vol. 25, no. 12, Dec 2020, doi: 10.1117/1.JBO.25.12.126005.

[14] C. Zhao et al., "Multimodal photoacoustic/ultrasonic imaging system: a promising imaging method for the evaluation of disease activity in rheumatoid arthritis," Eur Radiol, vol. 31, no. 5, pp. 3542-3552, May 2021, doi: 10.1007/s00330-020-07353-z.

[15] M. Yang et al., "Synovial Oxygenation at Photoacoustic Imaging to Assess Rheumatoid Arthritis Disease Activity," Radiology, vol. 306, no. 1, pp. 220-228, Jan 2023, doi: 10.1148/radiol.212257.

[16] M. Quigley et al., "ROS: an open-source Robot Operating System," in ICRA workshop on open source software, 2009, vol. 3, no. 3.2: Kobe, Japan, p. 5.

[17] U. Robots, "The urscript programming language," Universal Robots A/S, version, vol. 3, 2015.

[18] Z. Cao, T. Simon, S.-E. Wei, and Y. Sheikh, "Realtime multi-person 2d pose estimation using part affinity fields," in Proceedings of the IEEE conference on computer vision and pattern recognition, 2017, pp. 7291-7299.

[19] T. Simon, H. Joo, I. Matthews, and Y. Sheikh, "Hand keypoint detection in single images using multiview bootstrapping," in Proceedings of the IEEE conference on Computer Vision and Pattern Recognition, 2017, pp. 1145-1153.

[20] ZacharyTaylor, 2016. [Online]. Available: https://github.com/ZacharyTaylor/Camera-to-Arm-Calibration

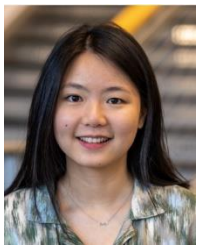

Xiaorui Peng received her B.S. degree in Electrical Engineering from Beijing Institute of Technology in 2019 and her master's degree in Biomedical Engineering from Duke University in 2021. Now, Xiaorui joined the Optical Imaging Laboratory and is pursuing her Ph.D. degree in Biomedical Engineering at the University of Michigan. Her current research interests focus on potential clinical applications of photoacoutics.

Aaron Dentinger (M'95) received his B.S. degree in engineering physics in 1992 and his M. S. and Ph.D. degrees in electrical engineering in 1994 and 2006, respectively, from Rensselaer Polytechnic Institute, Troy, NY., Since 1995, he has worked as an Electrical Engineer at GE Global Research in Niskayuna, NY and is currently a member of the Ultrasound and Biomedical Laboratory. Prior to joining GE, he was employed at Reveo, Inc. His current research interests are in ultrasound signal and image processing for vascular, cardiac, and physiological measurements.

Shivangi Kewalramani received her B.E. degree in Electronics and Communications from Birla Institute of Technology and Science, Dubai in 2019 and is pursuing a master's degree in Biomedical Engineering along with minor's in Data Science from University of Michigan. She has carried out research on photoacoustic imaging in the optical engineering area.

Zhanpeng Xu is a Ph.D. candidate from the Department of Biomedical Engineering, University of Michigan, Ann Arbor. He received his B.S. degree from Sichuan University and M.S. degree from Zhejiang University in China. His research interests focus on photoacoustic measurement and imaging, photoacoustic microscopy, hyperspectral imaging et al. He has published more than 10 peer-reviewed journal papers, and served as the independent reviewer for Optics Express, Optics Letters, Biomedical Optics Express, Progress in Electromagnetics Research, Applied Optics, and Plos One.

Steven Gray is a Lead Robotics Engineer at GE Research in Niskayuna, NY. His research interests include grasp and motion planning, robotics software architecture, and sliding-scale autonomy. He is responsible for robotic motion planning and control on GE Research'a Telerobotics effort, enabling remote robotic inspection under high latency connections.

He has previously worked on aerial inspection efforts using autonomous drones to monitor the health of industrial assets, writing the motion planning software behind Avitas Systems, a GE Venture. On the Vertex program with GE Aviation Systems, he led the software development on planning, mission orchestration, and world modeling to identify targets using a heterogeneous team of UAVs with a mixture of EO and software-defined radio (SDR) sensing.

Prior to joining GE Research in 2016, Dr. Gray solved problems in motion planning and control for humanoid robots on Lockheed Martin's team in the DARPA Robotics Challenge. He and GRC coworker Shiraj Sen took second place in the 2017 NASA Space Robotics Challenge, using a sliding-scale autonomy approach to enable a simulated R5 Valkyrie humanoid to accomplish maintenance tasks. This system was demonstrated on MIT's R5 in October 2017. Dr. Gray earned his B.S. in Mechanical Engineering from Caltech in 2007 and his M.S and Ph.D. from the University of Pennsylvania in 2010 and 2013, respectively, advised by Dr. Vijay Kumar in the General Robotics, Automation, Sensing, and Perception (GRASP) Laboratory.

Soumya Ghose holds a Master's in Computer Application degree from India and a Master's in Computer Vision and Robotics from Heriot Watt University, UK. He received his PhD degree in Computer Engineering – Medical Image Analysis from University of Dijon, France in 2012. He worked as a post-doctoral fellow in Australia's Commonwealth Scientific Research Organization on MR only radiation therapy planning for prostate cancer between 2012-2015. Soumya joined Case Western Reserve University in 2015 as a Senior Research Associate working with Prof. Anant Madabhushi on prostate cancer risk stratification from multimodal medical images. He joined GE Research as a Lead Scientist in AI and Computer Vision group in 2018. He is currently a Senior Scientist in GE Research working on several business and NIH funded projects. Soumya's research is focused towards developing novel machine learning, deep learning, segmentation, and registration methods applied to detection, prognosis prediction and treatment of diseases from medical images (Ultrasound, MR, CT, H&E and Autofluorescence images) and clinicopathological variables.

Yew Teck Tan received the B.S. degree in computer science in 2006, developing path planner for mobile robotic systems, and the M.Eng. and Ph.D. degrees in electrical and computer engineering in 2009 and 2014, respectively. Since 2019, he is the lead engineer in Robotics and Autonomous Systems group at General Electric Global Research Center. His research interests include path planning, system integration, machine learning, autonomy and robotics.

Zhaoyuan Yang received his B.S. and M.S. degree in Electrical and Computer Engineering in 2017 and 2018, respectively, from The Ohio State University, Columbus, Ohio. Since 2018, he has worked as a research engineer at GE Research in Niskayuna, NY and is currently a member of the computer vision lab. His current research interests are in robustness and uncertainty quantification for computer vision models.

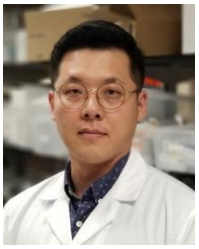

Janggun Jo received his B.S. and M.S. degree in Electronic Engineering from KoreaTech in Korea. He received his Ph.D. degree in Bioengineering at the University of Kansas. And Dr. Jo finished his postdoc fellowship at the University of Michigan. Currently he is a Research Investigator in the Department of Biomedical Engineering at the University of Michigan. His research interests include Photoacoustic imaging modality including Optical and Ultrasound imaging as well as high intensity focused ultrasound treatment.

David Chamberland received his B.S. in Electrical Engineering from the University of Portland and his M.D. from the Oregon Health Sciences University. He joined the University of Michigan in 2004 and has been working on medical applications of photoacoustic technology for over 15 years. His training in electrical engineering and also a long history of working as a clinical rheumatologist with board certifications in internal medicine and rheumatology enable him to help with translation of applications into the clinical space.

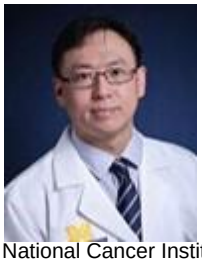

Guan Xu received his PhD and postdoctoral training in optical and ultrasound imaging in biomedicine. He received a predoctoral award from Congressionally Directed Medical Research Programs, a postdoctoral fellowship from American Heart Association, a Career Development Award from American Gastroenterology Association, a Senior Research Award from Crohn's and Colitis Foundation and an R37 MERIT award from National Cancer Institute.

Nada Abdulaziz received her medical degree from the University of Khartoum Faculty of Medicine. Her followship in Rheumatology was at the University of Michigan, where she pursued her career as Clinical assistant professor in Rheumatology Division. As a faculty member, she has been awarded W.J. (Joe) McCune Award for Teaching Excellence. She is currently a member in the fellowship Competency Committees that oversee the academic progression of rheumatology fellows across all phases of their training. She has an interest in inflammatory myositis diseases and is part of a multidisciplinary team in myositis program.

Girish Gandikota obtained board certifications in surgery (F.R.C.S.) and Radiology (F.R.C.R.) in the U.K. He did his fellowship in Musculoskeletal Radiology at McMaster University, Hamilton, Ontario, Canada. After the fellowship, he joined the University of Michigan as a lecturer. He has been promoted successfully to the professor and has received American board certification (A.B.R.). He has also obtained ultrasound R.M.S.K. certification from APCA/ARDMS.

Winner of the excellence in teaching awards, Dr. Gandikota has been an invited speaker, delivering more than 300 invited lectures and national presentations. He has over 75 scientific papers/exhibits in national conferences and over 68 peer-reviewed publications to date. His main research interests include M.S.K. Ultrasound, Sports Medicine, and Arthritis. Presently has over 15 years of M.S.K. ultrasound experience. Conducts C.M.E. courses on M.S.K. radiology and ultrasound in U.S.A. and India. He is a co-investigator in a NIH RO1 Grant ($3,545,507) on Arthritis. He has mentored many residents, fellows, technologists and medical students.

Dr. Gandikota recently joined us from the University of Michigan where he was Professor of Radiology. In addition to teaching and research, Dr. Gandikota had multiple administrative roles at the University of Michigan and at the national level. He was the Chair of Clinical Competency Committee, Radiology Residency Program, and in charge of M.S.K. resident training, curriculum development, and evaluation. He was also the Director, Domino Farms Radiology.

He is a member of national professional societies like the Radiological Society of North America (R.S.N.A.), American Roentgen Ray Society (A.R.R.S.), Society of

Skeletal Radiology (S.S.R.), and American Institute of Ultrasound in Medicine (A.I.U.M.), where he regularly lectures. He was the Chair of the Assessment Oversight Team (A.O.T.) RMSK-APCA appointed for the musculoskeletal physician examination. He is a reviewer for multiple esteemed radiology and rheumatology journals, including Arthritis and rheumatology.

David Mills (M'02) is a Principal Scientist in the Ultrasound and Bioinstrumentation lab at GE Research in Niskayuna, NY. He received the B.S. degree in engineering (summa cum laude) from LeTourneau University, Longview, TX, USA, in 1994, and the Ph.D. degree in biomedical engineering from Duke University, Durham, NC, USA, in 2000. He joined GE Research in 2000 where he is involved in the research and development of medical ultrasound transducers and advanced ultrasound applications. He has led multiyear research programs on ultrasound applications and drug delivery using microbubbles, including scan guidance and image analysis technology. He has authored many publications and conference presentations in these areas and holds more than 25 patents related to medical ultrasound. His current research interests include the design of medical ultrasound transducers of both piezoelectric and cMUT-based transducers and new clinical applications for ultrasound that are enabled by real-time 3-D ultrasound imaging, visualization algorithms, and customized user interfaces to meet specific user needs.

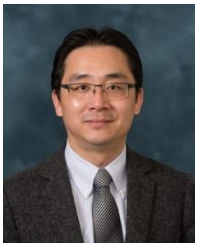

Xueding Wang is a Jonathan Rubin Collegiate Professor of the Department of Biomedical Engineering and the Professor of the Department of Radiology at the University of Michigan School of Medicine. Before working as an independent principal investigator, Dr. Wang received his Ph.D. at Texas A&M University and Postdoctoral training at the University of Michigan. Dr. Wang has extensive experience in development of medical imaging and treatment technologies, especially those involving light and ultrasound. Sponsored by NIH, NSF, DoD and other funding agencies, his research has led to over 160+ peer-reviewed journal papers. Dr. Wang was the recipient of the Sontag Foundation Fellow of the Arthritis National Research Foundation in 2005, the Distinguished Investigator Award of the Academy of Radiology Research in 2013, and was elected to the fellow of AIMBE in 2020 and the fellow of SPIE in 2021. He is also sitting on the editorial boards of scientific journals including Photoacoustics, Ultrasonic Imaging, Journal of Biomedical Optics, Medical Physics, and Scientific Reports.